

PROCEEDINGS OF SPIE

[SPIDigitalLibrary.org/conference-proceedings-of-spie](https://www.spiedigitallibrary.org/conference-proceedings-of-spie)

Helium ion active hybrid non-chemically amplified resist (n-CAR) for sub-10 nm patterning applications

Sharma, Satinder, Reddy, Pulikanti Guruprasad, Moinuddin, Mohamad Ghulam, Ghosh, Subrata, Pradeep, Chullikkattil, et al.

Satinder K. Sharma, Pulikanti Guruprasad Reddy, Mohamad Ghulam Moinuddin, Subrata Ghosh, Chullikkattil P. Pradeep, Kenneth E. Gonsalves, "Helium ion active hybrid non-chemically amplified resist (n-CAR) for sub-10 nm patterning applications," Proc. SPIE 10584, Novel Patterning Technologies 2018, 1058409 (19 March 2018); doi: 10.1117/12.2297537

SPIE.

Event: SPIE Advanced Lithography, 2018, San Jose, California, United States

Helium ion active hybrid non-chemically amplified resist (n-CAR) for sub-10 nm patterning applications

Satinder K. Sharma^{*1}, Pulikanti Guruprasad Reddy², Mohamad Ghulam Moinuddin¹, Subrata Ghosh², Chullikkattil P. Pradeep², and Kenneth E. Gonsalves^{** 2}

¹ School of Computing and Electrical Engineering, Indian Institute of Technology (IIT)-Mandi, (H.P), 175005, India.

² School of Basic Science, Indian Institute of Technology (IIT)-Mandi, (H. P), 175005, India.

ABSTRACT

Patterning of the resist features down to 10 nm node is crucial for futuristic integrated circuits (ICs) technology advancements. In this regard, we design and developed a novel hybrid non-chemically amplified resist (n-CAR) i.e. MAPDST-*co*-ADSM (where MAPDST = (4-(methacryloyloxy)phenyl) dimethylsulfonium trifluoromethanesulfonate and ADSM = (acetyldibutylstannyl methacrylate)) for high-resolution Helium Ion (He⁺) Beam Lithography (HIBL) studies. The developed resist exhibits the high sensitivity toward Helium ion radiation and patterned sub-15 nm features at the dose ~50 $\mu\text{C}/\text{cm}^2$ onto negative tone resist formulation. In order to recognize the critical dimension (CD), the resist thin films were analyzed for single pixel exposure dose analysis at He⁺ exposure dose ranging from ~30 pC/cm to ~100 pC/cm. These investigations apparently reveal that 10 nm single pixel line features of the MAPDST-*co*-ADSM resist is patterned with the dose ~50.48 pC/cm. The improved patterning resolution of the resist down to 10 nm is due to the inclusion of hybrid tin sensitizer in the resist structures. The MAPDST-*co*-ADSM showed coherent line edge roughness (LER) and line width roughness (LWR) values for 15 nm lines features as $\sim 1.67 \pm 0.27$ nm and ~ 2.20 nm respectively.

Monte Carlo-based simulation technique is a standard method for statistical analysis and modelling of stochastic processes; such as noise in circuits, carrier transport and study of ion implantation/interaction/trajectory on materials for integrated circuits. Thus Monte Carlo ion trajectory simulation for MAPDST-*co*-ADSM resist formulation showed that the negligible (~0.5%) target damage and recoil generation (atom displacement) of total energy delivered to the system (MAPDST-*co*-ADSM/Si) in novel HIBL exposure due to much larger stopping power of He⁺ ion and low proximity effect.

Keywords: Next Generation Lithography, Non-chemical Amplified Resist (n-CAR), He⁺ Beam Lithography (HIBL), Monte Carlo simulation, Higher Stopping Power & Sensitivity, LWR & LER, Sub-10 nm Patterning and Critical Dimensions (CD).

1. INTRODUCTION

Development of semiconductor devices down to ~7 nm or below process technology node is indispensable for modern semiconductor and analogous micro/nanoelectronic industries. Moore's Law (1965)^[1] is a key driving force for the remarkably cost reduction per transistor, higher transistor density, frequency, and functionality. To exhibit this trend for the next-generation microelectronic industry, continuous shrinking of the device feature size with industry-leading performances such as low leakage power, low voltage operation, high energy efficiency and reduction in cost per transistor is essential^[2]. Evaluation of novel patterning techniques and advanced photoresists technologies for lithography process is an active research area over the past 45 years for ICs miniaturization^[3]. To date, a large number of high-resolution lithography techniques include 193 nm immersion, Helium/Gallium ion beam, extreme ultraviolet lithography (EUVL, $\lambda = \sim 13.5$ nm), e-beam lithography etc., have been explored for 10 nm or beyond patterning applications^[4,5]. Out of these, He⁺ beam lithography (HIBL) received a significant interest from scientific and industry community due to potential patterning down to ~7 nm or below features using a high focused beam of He⁺ at the step size 0.5 nm with substantially low proximity effect^[6].

Corresponding Authors: ^{**}kenneth@iitmandi.ac.in; ^{*}satinder@iitmandi.ac.in

Recent reports state that e-beam lithography (EBL) unable to achieve such high resolution targeted, next generation critical dimensions due to subsequent backscattering and secondary electrons emission which induce the noteworthy proximity effect and consequently lead to the high-resolution pattern blurring and collapsing at 10 nm or beyond technology node.^[7] While the secondary electrons (SE_{HIBL}) generated in novel alternate HIBL technique entail the low energy (<10 eV) and localized in the incident beam path of He^+ source. Whereas, the EBL secondary electrons (SE_{EBL}) having higher energy (>100 eV), therefore, the high energy SE_{EBL} travel relatively long distance in the resist material and results in a broadening of the resist features as compared to the SE_{HIBL} .^[7] Furthermore, the stopping power of ions is much larger as compared to the electrons, which clearly reveals that more ions energy delivered onto few tens of nanometer thickness of resist and might be result the significant enhancement in resist sensitivity. Therefore, to counter the high-resolution sub-10 nm or beyond node patterning issues, rising from EBL, researchers developed a novel alternative high-resolution patterning HIBL technique with improved resolution and sensitivity^[8].

Moreover, HIBL compatible resists reports are quite rare as compared to EBL resists as described in the literature. To date, two commercial resists such as PMMA and HSQ have been used extensively for high-resolution HIBL studies^[6, 9, 10]. Shi *et al.* reported fullerene-based molecular non-chemically amplified resist (n-CAR) for sub-10 nm patterning applications by using 10 nm film thickness at the dose $\sim 40 \mu C/cm^2$ ^[11]. In addition, Feixiang Luo *et al.* developed Hafnium-based metal oxide resist $HfSO_x$ for sub-10 nm patterning studies with $\sim 2-4 \mu C/cm^2$ and low LER than the similar resist analyzed under EUVL and EBL^[12]. Very recently, we explored a new n-CAR resist MAPDSA-co-MAPDST for sub-20 nm patterning studies using HIBL technique with ultra-low sensitivity ($7.2 \mu C/cm^2$) and LER (1.27 ± 0.31 nm)^[13]. Therefore, in order to continue our extensive research on HIBL, in the present work we designed and developed a new hybrid n-CAR resist MAPDST-co-ADSM based on the radiation sensitive organic monomer MAPDST ((4-(methacryloyloxy)phenyl)dimethylsulfonium trifluoromethanesulfonate) and hybrid inorganic tin sensitizer ADSM (acetyldibutylstannyl methacrylate) for HIBL applications. We used MAPDST as a polarity render due to its ability to bring polarity conversions by changing the resist properties from hydrophilic to hydrophobic during the lithography process^[14]. The lithography performance of the developed resist formulation MAPDST-co-ADSM was investigated under He^+ beam with step size ~ 0.5 nm. Moreover, Monte Carlo ion trajectory simulation for the interaction of He^+ radiation with novel MAPDST-co-ADSM thin films has been performed to study the effect of a secondary electron and stopping power over the resist formulation, irradiated with He^+ radiation. The more details of these studies were discussed in the following subsections.

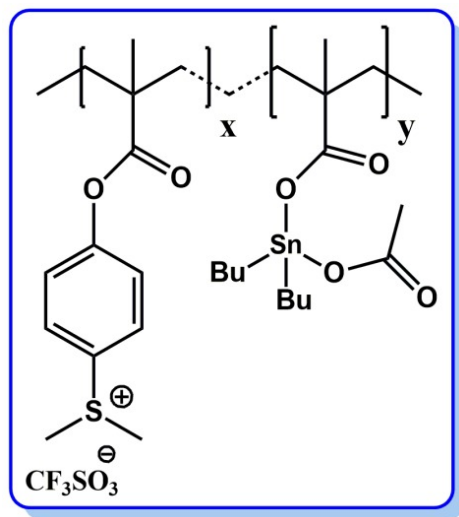


Figure 1. Chemical structure of MAPDST-co-ADSM copolymer resist for HIBL studies.

2. EXPERIMENTAL DETAILS

2.1 Resist formulation and thin film preparation

The hybrid copolymer resist MAPDST-*co*-ADSM was synthesized through free radical polymerization process by the reaction between starting organic monomer MAPDST and tin hybrid monomer ADSM by using AIBN as a free radical initiator in ACN/THF (1:1) at 65 °C for 2 days. The chemical structure of the MAPDST-*co*-ADSM was given in Figure 1. The synthesized polymer was thoroughly characterized by using the NMR, IR, GPC, TGA and EDX spectroscopic techniques. The calculated molecular weight (Mol. w) and poly-dispersity index (PDI) of the hybrid copolymer resist was 8221 g/mol and 1.51, respectively. The resist formulations were prepared by dissolving of the solid MAPDST-*co*-ADSM (2 wt %) copolymer in the acetonitrile solution followed by filtering through 0.2 µm Teflon filters in order to get a particle-free solution. The defect-free thin films with the thickness ~30 nm were achieved by spin coating of the resist solutions onto the 2-inch p-type silicon wafer at 4500 rpm speed for 60 sec. Later, the resist coated thin films were subjected to pre-exposure bake at 90 °C for 60 sec. After, He⁺ beam irradiation, the resist thin films were subjected to a post-exposure bake at 70 °C for 60 sec. Finally, the high resolution resist patterns were achieved after the development of resist thin films with aqueous 0.022N, TMAH developer solution for 30 sec.

2.2 He⁺ Beam irradiation of resists samples

The pre-baked resist thin films samples were subjected to He⁺ beam irradiation by using Zeiss ORION Nano Fab system available at Carl Zeiss Microscopy, Peabody (USA) with the Gas Field Ion Source (GFIS) for 10 nm patterning investigations. Helium ion beam radiation with virtual probe size 0.5 nm and aperture 7 µm (for acceleration of 30 KeV) were used for these studies. He⁺ beam at 30 KeV acceleration voltage held to preserve the beam current of 1 pA while keeping the dwell time as a variable for different dose exposure. The single pixel exposure for critical dimension (CD) of the resist was performed with pixel spacing 1 nm (Figure 2). Various helium ion doses starting from 30 pC/cm-100 pC/cm was examined for high-resolution single pixel line patterning of the L-shaped ~10 nm features.

2.3 Monte Carlo simulation

Monte Carlo based algorithm is widely used to simulate many of the stochastic processes such as noise in circuits, carrier transport in sub-micron devices and study of ion implantation/interaction/ion trajectory on materials. Monte Carlo simulation analysis is a powerful tool for understanding ion behaviour in ion beam microscopy^[15]. This technique is used in many of the tools available in the market such as in SPICE, ATHENA and ATLAS -process and device simulators respectively and SRIM (Stopping and Range of Ions in Matter) for simulating ion transport in resist materials such as stopping power, ion range and its straggling distributions etc. In the case of ion transport simulation Monte Carlo programs calculate a large number of individual ion trajectories in targeted resist materials. Each particle history begins with a random starting position within the implantation window, a given direction, and an ion beam energy. This technique can be employed wherever energetic ions and resist materials interactions and encountered. This technique uses appropriately scaled random numbers, and hence the accuracy of results obtained with the Monte Carlo method depends on sample size and hence large computation time. The ion-induced secondary electrons and their contribution in changing the polarity of n-CAR such as MAPDST-*co*-ADSM have been studied by Stopping and Range of Ion in Matters based on Bragg's law^[16]. Bragge *et al.* postulated that the stopping power of a material may be estimated by the linear combination of the stopping powers of its individual elements of that material^[16,17]. To compare Helium ion beam with existing e-beam, CASINO V. 2.48 (Monte Carlo simulation of electron trajectory in solids) was used to simulate e-beam trajectories in MAPDST-*co*-ADSM^[18]. Both simulations were performed based on 5600 trajectories and 30 KeV beam energy to compute same film model as examined under HIBL.^[08] In CASINO (electrons transport), a 0.5 nm beam size was set to have a comparable beam size with helium ion used experimentally.

3. RESULTS AND DISCUSSION

3.1 Dose optimization test

The smooth resist thin films with the thickness ~ 30 nm were characterized by using HR-AFM and line profilometer tools. The calculated RMS roughness for the MAPDST-co-ADSM resist thin films was ~ 0.55 nm, indicate that suitable resist thin films for nano-patterning studies.

In order to optimize the exposure dose for 10 nm patterning studies, initially the resist thin films were exposed to single pixel line patterning. The various He^+ doses starting from 30 pC/cm to 100 pC/cm were considered for the L-shaped (Ls) patterning as shown in Figure 2. These dose test analyses clearly reveal that 50 pC/cm is the minimum exposure dose required for patterning of the defect-free L-shaped features (10 nm) of the resist onto the silicon wafer (Figure 2 (c)). As shown in Figure 2, the thickness of the resist thin films was increasing gradually with the exposure dose, indicate that negative tone nature of the resist formulation. At the given exposure doses the developed patterns appeared as the shadow of resist (patterns for 30pC/cm shown in Figure 2 (a)). This might be due to given dose characteristics for ~ 10 nm patterning investigations are not enough, therefore, the resist thin films were washed away with the developer. While the discontinued L-shaped patterns exhibited by the resist formulation at the dose 40 pC/cm indicate that further enhancement of dose is necessary for collapse free nano-patterning (Figure 2 (b)).

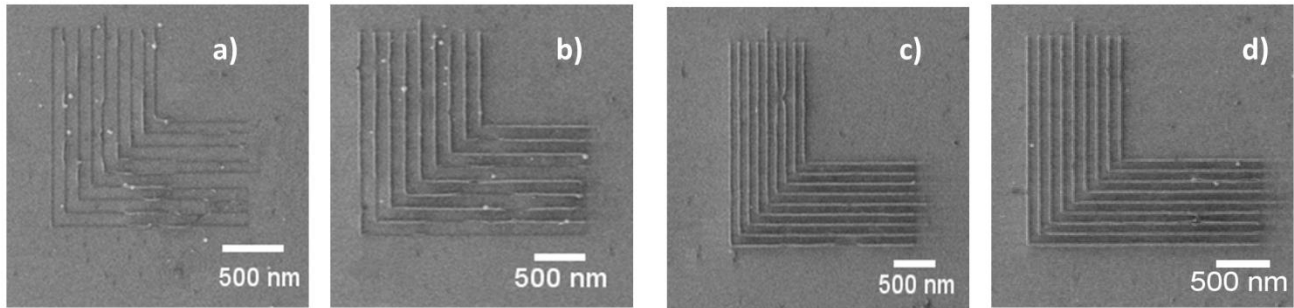


Figure 2 Dose test analysis of single pixel line patterns of the L-shaped features obtained from the MAPDST-co-ADSM resist at various doses (a) 30pC/cm, (b) 40 pC/cm, (c) 50 pC/cm, and (d) 100 pC/cm.

The L-shaped arrays of single pixel line patterns generally define the line edge sharpness and point spread function of a resist^[6]. The L-shaped ~ 10 nm features with different line spacing (150 and 200 nm) exhibited by the resist at doses 50.6 and 101.2 pC/cm was shown in Figure 3(a). The zoomed L-shaped patterns of the resist at the dose 50 pC/cm were shown in Figure 3(b). Further, in order to measure the critical dimension of these resist patterns, the resist thin films were subjected to intensity contrast spectra analysis. The calculated critical dimension (CD) of the L-shaped resist patterns is ~ 10.5 nm (Figure 3(c & d)). These findings reveal that our newly designed and developed resist formulation has a potential to pattern 10 nm and below features at the given experimental conditions.

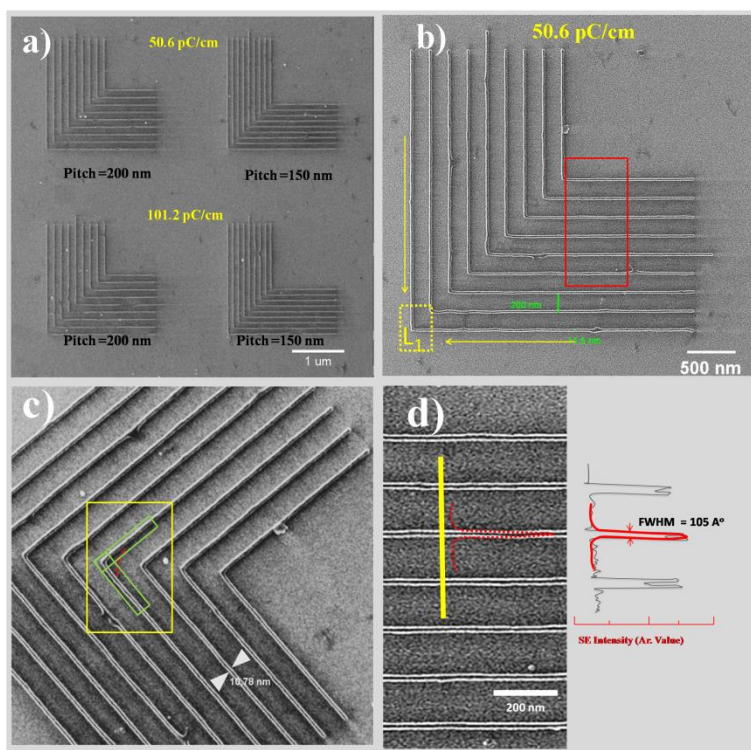


Figure 3 a) He^+ exposed L-shaped ~ 10 nm patterns of the MAPDSA-*co*-ADSM resist with different pitch (150 and 200 nm) and doses (50 and 100 pC/cm); b) Zoomed image of L-shaped patterns exhibited by the copolymer resist at the dose 50 pC/cm; c) The image showing line edge sharpness and overlapping area of single pixel L-shaped features; d) contrast spectra analysis for CD measurements of the patterned L-shaped features.

3.2 Pattern analysis

Further, the sub-15 nm line features exhibited by the MAPDST-*co*-ADSM resist formulation was characterized by using He^+ Zeiss ORION Nano microscope. The high resolution 15 nm line patterns with various line/space characteristics such as L/10S, L/5S, L/4S and L/2S patterned from the resist formulation at the dose $50 \mu\text{C}/\text{cm}^2$ are shown in Figure 4 (c-f). As perceived from the Figure 4 (c-f), the 15 nm line patterns are well developed and resolved; no pattern buckling, deformation is observed under the given experimental conditions. Whereas, the ability to L/S (line/space) ~ 15 nm features are unsuccessful at this stage due to buckling and patterns collapsing (not shown here). In order to find out the line edge roughness (LER) and line width roughness (LWR), the patterned resist thin film images were subjected to SuMMITTM metrology calculations. The calculated LER and LWR parameters for 15 nm L/10S, L/5S and L/4S (line/space) features were 1.67 nm, 2.2 nm; 2.85 nm, 4.05 nm and 3.62 nm, 4.42 nm respectively. This computation, the LER and LWR parameters increasing gradually with the resolution of the patterned features from L/10S to L/2S. Therefore, resist resolution influence the LER and LWR parameters. The LER and dose values reported for sub-15 nm features exhibited by the resist is better/comparable to some of the helium ions resists reported in the literature^[12].

Similarly, the high resolution 10 nm line features with L/10S and L/5S (line/space) characteristics obtained from the developed resist formulation is showed in Figure 4 (a & b). Like sub-15 nm features, the ~ 10 nm features of the resist with high-resolution patterns such as L/4S to L/S (line/space) are not well resolved, might be due to the resolution limit of the developed resist formulation. The calculated LER and LWR parameters for exposed 10 nm L/10S and L/5S (line/space) features were 2.01 ± 0.47 nm, 2.98 nm and 2.6 ± 0.11 nm, 3.95 nm, respectively.

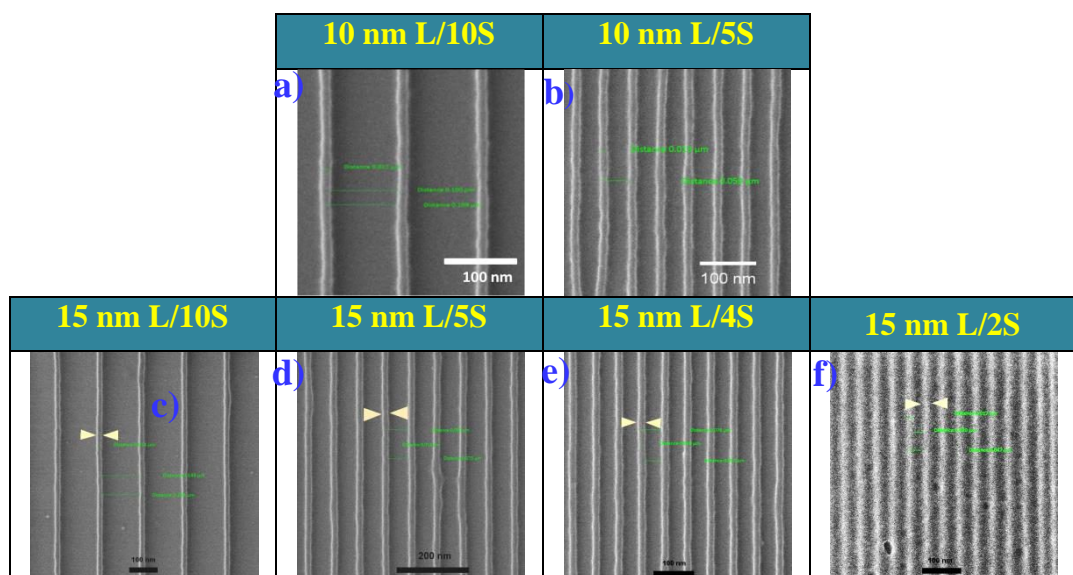


Figure 4 (a-b) 10 nm line patterns with L/10S and L/5S features of the MAPDST-*co*-ADSM resist at the dose 50 $\mu\text{C}/\text{cm}^2$ (c-f) Pattern analysis of 15 nm line features with different line/space characteristics (L/10S to L/2S) exhibited by the copolymer MAPDST-*co*-ADSM resist at the dose 50 $\mu\text{C}/\text{cm}^2$.

As known, sulfonium triflates based resists are highly sensitive to light and radiations. The major part of the MAPDST-*co*-ADSM copolymer consist the radiation sensitive sulfonium triflates of MAPDST. During the He^+ irradiation based HIBL process, the radiation sensitive MAPDST undergoes structural conversations from polar sulfonium triflates to non-polar aromatic sulfide functionality. Therefore, the newly developed resist formulation offering the high resolution, negative tone features upon the developing of the exposed resist thin films with aqueous hydrophilic developer solution such as TMAH. Since, TMAH dissolves essentially the unexposed portion of the resist patterns, while leaving the exposed resist portion on the Si wafer. The inorganic ADSM was included in the resist structure in order to improve the resist sensitivity and resolution. The ADSM consist the high energy harvesting tin (Sn) metal with the high optical density (8-10) than compared to the carbon (0.2). Our previous reports on poly(MAPDST) resist for EBL and EUVL studies reveal that patterning of sub-20 nm features was achieved with moderate sensitivity.

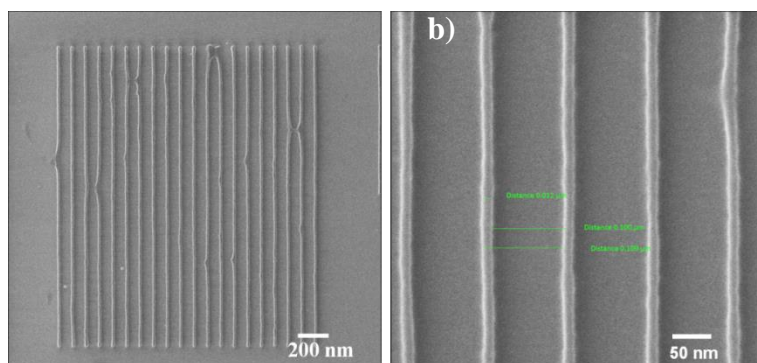


Figure 5 A 10 nm line pattern with 50 $\mu\text{C}/\text{cm}^2$ a) overview b) high-resolution HIM images at 50 nm scale bar.

Due to the inclusion of ADSM in the poly(MAPDST), the resist sensitivity of the MAPDST-co-ADSM got enhanced from sub-20 nm to ~10 nm features with improved next-generation lithography properties (shown in Figure 5). This is the desirable outcome of this study. Moreover, sulfonium triflate based resists well explored for wide range lithography tools but their patterning efficiency toward novel HIBL studies are not explored yet.

3.3 Simulation analysis

In high-resolution patterning, using EBL, we deal with giant proximity, blurring effect and also influenced by different degrees of deterioration due to secondary electrons and lower stopping power. The secondary electrons generated in the path of incident e-beam inside the few nanometers thickness of top resist layers travels in the plane and result in the high-resolution pattern destruction, buckling and even in worse case patterns collapse^[19]. The effect of SE_{EBL} over the charge based lithography has been extensively reported, it is also observed that for SE_{HIBL} also affect the high resolution resist patterns topology and sensitivity extensively^[12,15]. Here, the ion trajectory inside the resist material with very low energy (<10 eV) for 30 KeV, He^+ beam interaction with newly developed MAPDST-co-ADSM (light photoresist with low Mol. weight ~8221 gram/mol in comparison of PMMA Mol. weight 22,000 gram/mol) is computed.

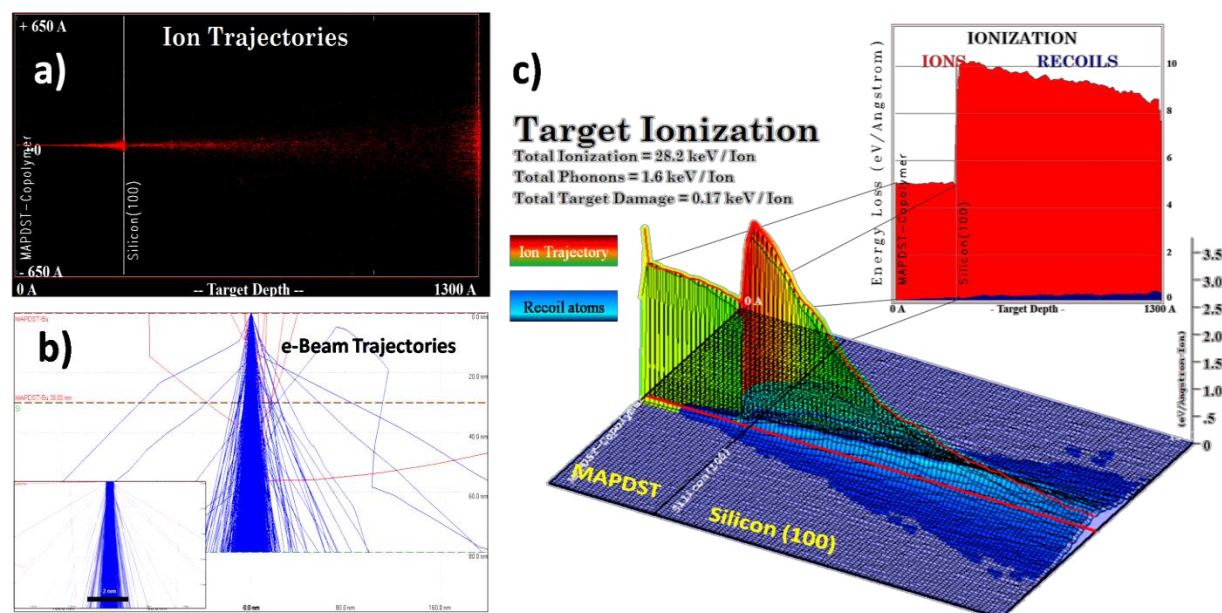


Figure 6 Charge particle trajectory inside the MAPDST co-polymer layer a) He^+ ion trajectory with less deviation than b) e-beam trajectory in MAPDST with 5 Å beam spot (beam spreading inside the MAPDST-co-ADSM layer); c) 3D Target (MAPDST-co-ADSM/Si) ion distribution plot c*) Energy loss spectra (red) with recoil atoms (blue).

The simulated the normalized trajectory of He^+ ion as well as e-beam in MAPDST-ADSM, show the He^+ (Figure 6(a)) are more localized to the mean path in contrast to the e-beam irradiation (Figure 6 (b)). Here, Electron beam trajectory interaction with newly developed MAPDST-co-ADSM, Monte Carlo simulation is performed in Casino V. 2.48) at the same acceleration of 30 KeV. From our HIBL study optimum exposure dose for MAPDST-co-ADSM is $D_{100} = 50.6 \mu C/cm^2$ which is analogous to $3.25 \text{ ion}/nm^2$ as discussed in literature^[20,12]. Recent reported, experimental and simulation study for He^+ ion irradiation with different dose showed that no defect generation was found at $3.25 \text{ ion}/nm^2$ ($3.25 \times 10^{14} \text{ ion}/cm^2$) irradiation for silicon^[21]. Further, it was required to find the defect generation in MAPDST-co-ADSM with He^+ ions, which lead to pinhole formation and broadening LER/LWR^[20, 22]. Monte Carlo, TRIM (TRansport of Ions in Matter) analysis was executed to study the ion

interaction inside the resist (Figure 6.c). The simulated target ionization profile for 30 KeV showed that 92% of the total energy loss was utilized for target (MAPDST 300 Å / Silicon 1000 Å) activation which further initiates the production of secondary electrons. Figure 6.c* shows the He⁺ absorbance loss/Å in MAPDST-co-ADSM/Si(100) for 28.2 KeV (92%). Average of 5 eV/Å energy loss were spotted in 300 Å thick MAPDST-co-ADSM considering avg. molecular weight and density 8000-9000 and 1.634 gm/cm³ respectively. Therefore, the total energy dissipation of 1.5 KeV in 300 Å (30 nm), MAPDST layer. Further considering the SE emission estimation by Petrov *et al.* average energy of secondary electron are 1.6 eV (1 eV×1, 2 eV×0.8, 4 eV×0.5 and 5 eV×0.35) and total ~940 SE are generated by one 30 KeV He⁺ ion in MAPDST layer [23]. Moreover, from experimental data D₁₀₀ = 50 µC/cm², i.e it need ~ 3000 secondary electrons/ nm² to change the polarity of n-CAR.

In our charge trajectory study, we found that number of SE_{HIBL} required to expose the MAPDST-co-ADSM is much higher than the produced one, which nullifies the proximity effect. On other hand in e-beam lithography, the secondary electrons generated with ~100 eV energy will affect at a much higher rate than He⁺ ion beam lithography. Generally, the ion beam is used for direct patterning and etching purpose using heavy ion beam but while using He⁺ ion in comparison with Ga⁺ ion it is shown that the number of scattered electrons (1 %) and recoil atoms (0.5%) are very less which suggests a damage free nanopatterning with MAPDST-co-ADSM.

4. CONCLUSION

In summary, we have developed a novel organic-inorganic hybrid resist MAPDST-co-ADSM for higher resolution helium ion beam lithography studies. The developed resist formulation showing the well-developed and patterns sub-15 nm (L/10S to L/2S) features at the He⁺ dose 50 µC/cm². The single pixel dose analyses reveal that patterning of critical dimension features of the developed hybrid resist at the dose of ~50 pC/cm. In best experimental conditions the resist showed acceptable LER and LWR parameters for 15 nm features as ~1.67±0.27 nm and ~2.20 nm respectively, which are comparable or better than some of the helium ion resists reported in the literature. Monte Carlo, ion trajectory simulation for MAPDST-co-ADSM resist was studied to explain the effect of a secondary electron and stopping power over the developed resist formulation, irradiated with He⁺. The ionization study shows that negligible (~0.5%) target damage and recoil generation (atom displacement) of total energy delivered to the system. Therefore, MAPDST-co-ADSM is a potential candidate for HIBL with sub-10 nm features, low LER/LWR and high sustainability.

5. ACKNOWLEDGEMENT

Authors thank the Department of Science and Technology (DST) and Technology Systems Development Program (TSDP), India for the financial support. Sanctioned project reference number: DST/TSG/AMT/2015/634. P. G. Reddy thanks the Council of Scientific and Industrial Research (CSIR), New Delhi, India for a senior research fellowship. M. G. Moinuddin thanks the Ministry of Electronics & Information Technology for a junior research fellowship under the Visvesvaraya Ph.D Scheme. We are also thankful to HIM centre, Carl Zeiss Microscopy, Peabody (USA) for their constant technical support.

REFERENCES

1. Moore G. *Electronics Magazine*. Apr;38(8):114. (1965) (1965).
2. ITRS. "International Technology Roadmap for Semiconductors 2.0: Executive Report". *Int. Technol. roadmap Semicond.* 79 (2015).
3. Ito, T. & Okazaki, S. "Pushing the limits of lithography." **406**, 1027–1031 (2000).
4. Gangnaik, A. S., Georgiev, Y. M. & Holmes, J. D. "New Generation Electron Beam Resists: A Review." *Chem. Mater.* **29**, 1898–1917 (2017).
5. Blumenstock, G. M., Meinert, C., Farrar, N. R. et al. No Title. *Adv. Microlithogr. Technol.* **5645**, 188–195 (2005).

6. Winston, D. *et al.* "Scanning-helium-ion-beam lithography with hydrogen silsesquioxane resist." *J. Vac. Sci. Technol. B Microelectron. Nanom. Struct.* **27**, 2702 (2009).
7. Hlawacek, G., Veligura, V., van Gastel, R. & Poelsema, B. "Helium Ion Microscopy." 1–16 (2013). doi:10.1116/1.4863676
8. Watt, F., Bettiol, A. A., Van Kan, J. A., Teo, E. J. & Breese, M. B. H. "Ion beam lithography and nanofabrication: A review". *Int. J. Nanosci.* **4**, 269–286 (2005).
9. Ryssel, H., Habberger, K. & Kranz, H. "Ion beam sensitivity of polymer resists." *J. Vac. Sci. Technol.* **19**, 1358–1362 (1981).
10. Sidorkin, V. *et al.* "Sub-10-nm nanolithography with a scanning helium beam Sub-10-nm nanolithography with a scanning helium beam." **18**, 18–21 (2014).
11. Shi, X. *et al.* "Helium ion beam lithography on fullerene molecular resists for sub-10 nm patterning." *MEE* **155**, 74–78 (2016).
12. Luo, F., Manichev, V., Li, M. & Mitchson, G. "Helium ion beam lithography (HIBL) using HafSO_x as the resist." *Proc. SPIE* **9779**, 9779281–9779289 (2016).
13. Reddy, P. G. *et al.* "Heavy metal incorporated helium ion active hybrid non-chemically amplified resists: Nano-patterning with low line edge roughness." *AIP Adv.* **7**, 0–9 (2017).
14. Reddy, P. G. *et al.* "Design, development, EUVL applications and nano mechanical properties of a new HfO₂ based hybrid non-chemically amplified resist." *RSC Adv.* **6**, 67143–67149 (2016).
15. Stanford, M. G., Lewis, B. B., Mahady, K., Fowlkes, J. D. & Rack, P. D. "Review Article: Advanced nanoscale patterning and material synthesis with gas field helium and neon ion beams." *J. Vac. Sci. Technol. B, Nanotechnol. and Microelectron. Mater. Process. Meas. Phenom.* **35**, 30802 (2017).
16. Ziegler, J. F., Ziegler, M. D. & Biersack, J. P. "SRIM - The stopping and range of ions in matter (2010)." *Nucl. Instruments Methods Phys. Res. Sect. B Beam Interact. with Mater. Atoms* **268**, 1818–1823 (2010).
17. Bragg WH, K. R. X. "On the α particles of radium, and their loss of range in passing through various atoms and molecules." *London, Edinburgh, Dublin Philos. Mag. J. Sci.* **Sep 1;10(5)**, 318–40. (1905).
18. Drouin, D., Couture, A. R., Joly, D. *et al.*, "C. CASINO V2.42 - A fast and easy-to-use modeling tool for scanning electron microscopy and microanalysis users., *Scanning* **29(3)**, 92–101
19. Chang TH. Proximity effect in electron beam lithography. *J. Vac. Sci. Technol.* **Nov;12**, 1271–5. (1975).
20. Winston, D. *et al.* Neon ion beam lithography (NIBL). *Nano Lett.* **11**, 4343–4347 (2011).
21. Livengood, R., Tan, S., Greenzweig, Y., Notte, J. & McVey, S. Subsurface damage from helium ions as a function of dose, beam energy, and dose rate. *J. Vac. Sci. Technol. B Microelectron. Nanom. Struct.* **27**, 3244 (2009).
22. Pease, G. H. K. and R. S. The Displacement of Atoms in Solids by Radiation. *Reports Prog. Phys.* **18**, 1 (1955).
23. Petrov, Y. & Vyvenko, O. <title>Secondary electron emission spectra and energy selective imaging in helium ion microscope</title>. *Proc. SPIE - Int. Soc. Opt. Eng.* **8036**, 80360O–80360O–10 (2011).